УДК 629.7.02: 620.191.3.001.57

O.G. KUCHER[1], V.V. KHARYTON[2], J.-P. LAINE[2], F. THOUVEREZ[2]

[1] *National Aviation University, Aeroengines department, Ukraine*
[2] *Ecole Centrale de Lyon, Laboratory of Tribology and System Dynamics, France*

DETECTION OF CRACKED BLADE FROM BLADED DISK FORCED RESPONSE USING TIP-TIMING METHOD: SIMULATION STUDY

The study intends to simulate the process of the blade tip amplitude calculation by the tip-timing method. An attention is focused on tip-timing measurements for identification of a cracked blade from the bladed disk forced response. The cracked blade is considered within frameworks of the bladed disk dynamic model that takes into account mistuning presence. Nonlinear formulation of a crack behavior is done with the harmonic balance method in its combination with the contact analysis that allows simulation of crack breathing. In order to make the cracked blade identification process evident, the crack length and location are set in such a way as to produce the cracked blade frequency localization. Reconstruction of the blade tip amplitudes is attained with the arriving time of measured probes of the blade tips. The results are compared with the blade forced response obtained by the bladed disk dynamic model. Proposed model can be used for the simulation of the process of on-line health monitoring of aviation gas-turbine engines. And more particularly to provide data of engine vibration parameters modification in operation.

Key words: *cracked blade, bladed disk, forced response, tip-timing method.*

1. Introduction

Commonly known failure mode of aircraft gas-turbine engines is a high-cycle fatigue of turbine and compressor blades. It is caused by dynamic loading resulting in resonance blade vibration within operating range of rotor frequency. Most of engine shut-downs are caused by blade failures due to resonance vibration or flutter. Vibration-based inspection of structural behavior offers an effective tool of non-destructive testing. An analysis of forced response of a cracked structure to excitation forces and monitoring of alterations, which occur during its lifetime, may be used as a general integrity-assessment technique for detection of a crack presence.

A review of experimental studies allows drawing a conclusion that a decrease of natural frequencies of the beam-like model of the cracked blade is a major derived diagnostic sign. There are some approaches to inspect the vibration response of structures with non-propagating crack by means of stochastic analysis, examination of acoustic signals and a use of its frequency or modal data [3], [6], [16]. Structure displacements in the time domain can also provide information about crack presence [12], [13]. A study of crack effects within frameworks of the bladed disk is a complex problem and has been described in [18].

Health monitoring of the aviation engine requires relevant information about blade vibration. The information can be gathered through measurement of the blade dynamic performance. Usually vibration measurement is made with strain gauges mounted on the blade surface [7], [14]. The testing signal is received by a wireless telemeter system [17]. The technique allows continuous capture of responses from the selected blades. However, mounting of the system is a costly procedure as well as the system itself that must withstand centrifugal forces and high temperatures. It provides only few data points simultaneously.

Nowadays, some non-invasive methods, that attract increasing attention of the researchers, are based on measurement of blade tip deflections making use of the blade tip arriving time when a blade tip passes the probes stationary installed on engine casing. The technique is known as the tip-timing method [2], [5], [20], [21]. If there is no vibration, the blade tip arriving time depends only on the rotor rotation speed, while under vibration, it depends on vibration amplitude as well. The tip-timing method can be used to create an on-line system for monitoring the blade dynamic performance. The system should enable to solve the following tasks:

– initial data measurements (time of blade tip passing through the probe) using single- or multiprobes measurements

– calculation of characteristic parameters (vibration amplitude, blade tip deflection) using measured data

– processing of characteristic parameters in order to describe a selected blade dynamic behavior.

2. Bladed disk model subjected to tip-timing measurements

Simulation of the bladed disk forced response can be used to describe an application of tip-timing method.

Usually, the bladed disk dynamic problems are themselves the objects for application of the cyclic analysis technique. It is due to their behavior symmetry in circumferential direction. The presence of mistuning, i.e. a spread of structural properties from one blade to other, or in cyclic representation among the sectors, disrupts the symmetry. Though, an opportunity remains to continue cyclic analysis of the mistuned bladed disks [1]. The study deals not only with the mistuning caused by manufacture inequalities. The crack presence in the blade induces its nonlinear behavior that leads to impossibility to use cyclic analysis and a full-assembled disk model is required to simulate the crack effects on the disk forced response.

The finite elements model of disk sector with a cracked blade was initially developed using ANSYS (fig. 1, a). Then its structural matrices were transferred to MATLAB to continue sequential assembling process of the full bladed disk. As the initial data, a bladed disk with 31 blades was taken (fig. 1, b) with the same material properties for blades and disk (Young's modulus = $2 \cdot 10^{11}$Pa, Poisson's ratio = 0.3 and mass density = $7.8 \cdot 10^{3}$kg/m^3). Geometrical data of the model: disk radius = 0.3m, blade height = 0.08m, blade thickness in root section = 0.006 m, blade width in root section = 0.03 m, crack length = 0.004m (13.3% cracked blade), twisting angle = 30 deg. Excitation force amplitude = 0.3N.

Reduction of the model was suggested to be achieved by making use of a sub-structuring aProach. Crack location is assumed to represent an interface between two sub-structures. This is not a classical sub-structuring as these sub-structures are not entirely independent. In the case of the bladed disk, the model reduction is done on the base of a disk sector with a cracked blade. The sector is reduced and then the complete system assembling is performed.

For reduction the fixed-interface method is applied [4]. The fixed interface modes are the modes of the structure uncracked state and static modes are the modes of the crack opening. Relative displacements between contact pairs are considered as the interface or master DOFs. A certain number of modes describing uncracked bladed disk behavior and DOFs of nodes of external forces application are added to this set. The initial full model of the assembled bladed disk contained 28284 DOFs. It was reduced to the model with 136 master DOFs plus certain number of additional modes. It is sufficient to retain 50 additional modes to accurately approximate dynamic behavior of the full model within the range of the 1st blade flexural modes.

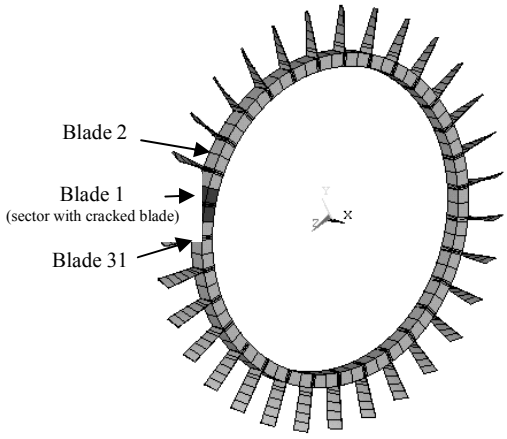

a

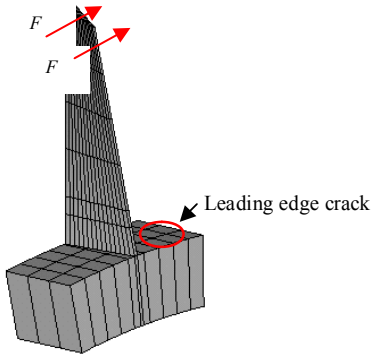

b

Fig. 1. Bladed disk finite element model:
a – assembled disk model, b – sector with a cracked blade

2.1. Nonlinear formulation of cracked blade behavior

Let the cracked blade nonlinear dynamic behavior be described by the equation of motion:

$$\mathbf{M}\ddot{\mathbf{u}} + C_{\xi}\dot{\mathbf{u}} + \mathrm{K}\mathbf{u} + \mathbf{F}_{\mathrm{nl}}(\mathbf{u}_{\mathrm{nl}}, t) = \mathbf{F}_{\mathrm{ext}}(t), \qquad (1)$$

where $\mathbf{u}$ is the vector of nodal displacements, $\mathbf{M}$, $\mathbf{C}_{\zeta}$, and $\mathbf{K}$ are symmetric mass, damping, and stiffness matrices of the bladed disk model, $\mathbf{F}_{\mathbf{ext}}$ is the vector of amplitudes of external excitation forces, $\mathbf{F}_{\mathbf{nl}}$ is nonlinear forces vector. Damping matrix was calculated on the base of structural damping ratio ξ and stiffness matrix $\mathbf{C}_{\zeta} = \xi\mathbf{K}$.

Nonlinear formulation of the problem under consideration can be done by means of the harmonic balance method. Detailed description of the procedure is given in [12], where the uncoupled cracked blade of the same geometry was studied. In accordance with the abovementioned procedure, a solution to equation (1) can be decomposed into the infinite base of trigonometric functions. Numerically, it is not rational to process the infinite sum and hypothesis that solution can be approximated by truncated Fourier series is applied.

Nonlinear and linear solutions in the time domain are shown for relative vertical displacement between two coinciding contact nodes – "crack point" (fig. 2) and horizontal displacement of excitation force application node – "tip point" (fig. 3). Simulations were performed at excitation frequency of 3410 rad/sec. The frequency is close to the resonance frequency of all-blades principal response (fig. 4).

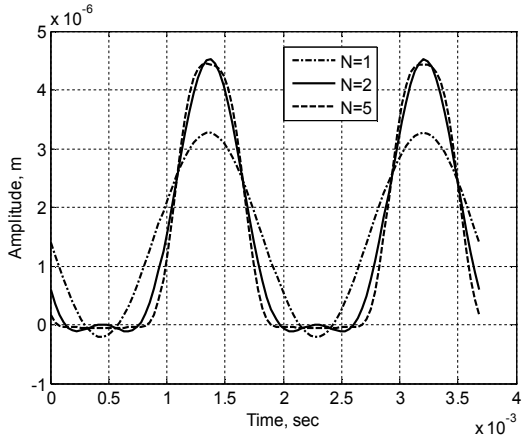

Fig. 2. Nonlinear solution by harmonic balance method for different harmonic numbers in "crack point"

Results of contact interaction simulations (fig. 2) reveal presence of the contact force. The set value of penalty stiffness (k_{nl}=10^{10} N/m) is sufficient to avoid penetration. Nonlinear force approximation allows accurate simulation of the nonlinear behavior of the cracked blade [11], [12].

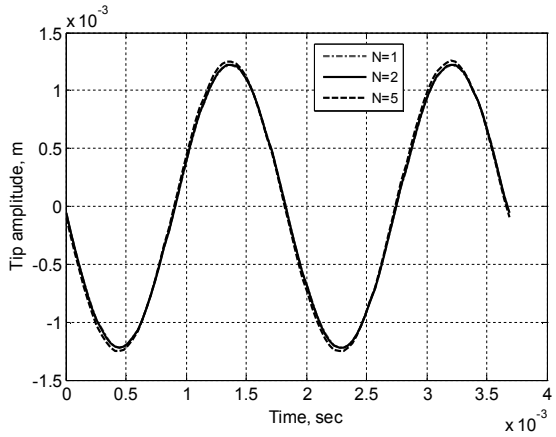

Fig. 3. Nonlinear solution by harmonic balance method for different harmonic numbers in "tip point"

Figs. 2–3 show the simulations performed for different numbers of retained harmonics. Their number is strongly critical to reduce computation time. For all following simulations the nonlinear model with two harmonics will be used as it provides a sufficient description of the system behavior. Besides, the blade tip response (fig. 3) remains practically sinusoidal and this can be used to simplify formulation of the tip-timing method governing equation [7], [20].

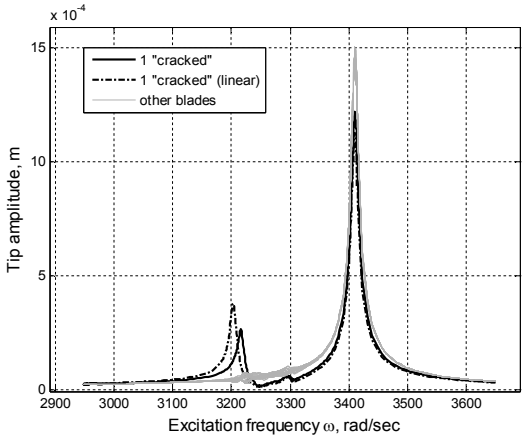

Fig. 4. Forced response of the bladed disk calculated at the "tip point" (crack length a=4mm)

The bladed disk frequency response (fig. 6) shows a notable difference between the linear and nonlinear responses measured for the cracked blade. During the crack closure an added energy dissipation is expected that results in lower magnitude of the cracked blade at its nonlinear formulation. The nonlinear formulation of the crack presence leads to the cracked blade localized resonance to be shifted to all-blades principal response as the nonlinear solution takes intermediate position between linear solution and solution to the uncracked blade [12]. It will probably cause problems with the cracked blade identification at certain level of mistuning. In addition, the cracked blade frequency localization is observed in fig. 6 (appearance of the additional peak).

2.2. Mistuning effect on forced response of the bladed disk model

Many authors admit that prediction of mistuning effect on the bladed disk response is a challenging problem [1], [15]. The difficulties are caused by two main complications:

– mistuning disrupts system cyclic symmetry, and

– mistuning leads to higher than expected amplitudes.

Mistuning effect on the bladed disk forced response can be represented by the blade stiffness mistuning. As far as the range of blade first flexural modes is considered in the analysis, the mistuning model can be represented by perturbation of the individual blade partition of the bladed disk stiffness matrix:

$$\mathbf{K}_j^{bm} = (1 + m_j)\mathbf{K}_j^{b}, \qquad (2)$$

where m_j is the mistuning coefficient of j-th blade relatively to the 1st blade (cracked) and randomly generated by normal law with mean μ=0 and standard deviation σ.

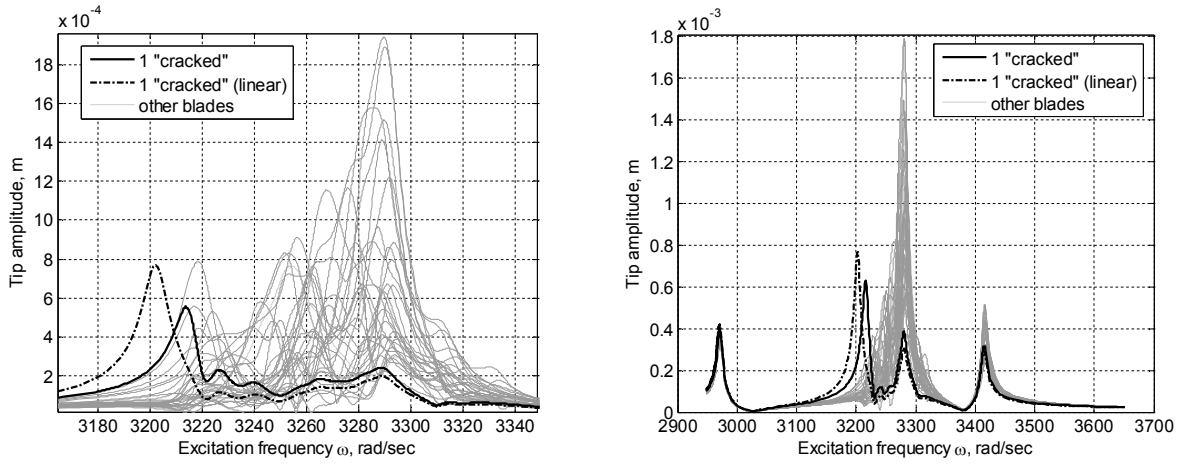

a b

Fig. 5. Mistuning effect on the bladed disk forced response (crack length a=4mm, EO=28):
a – σ=0.01; b – σ=0.01 (zoom)

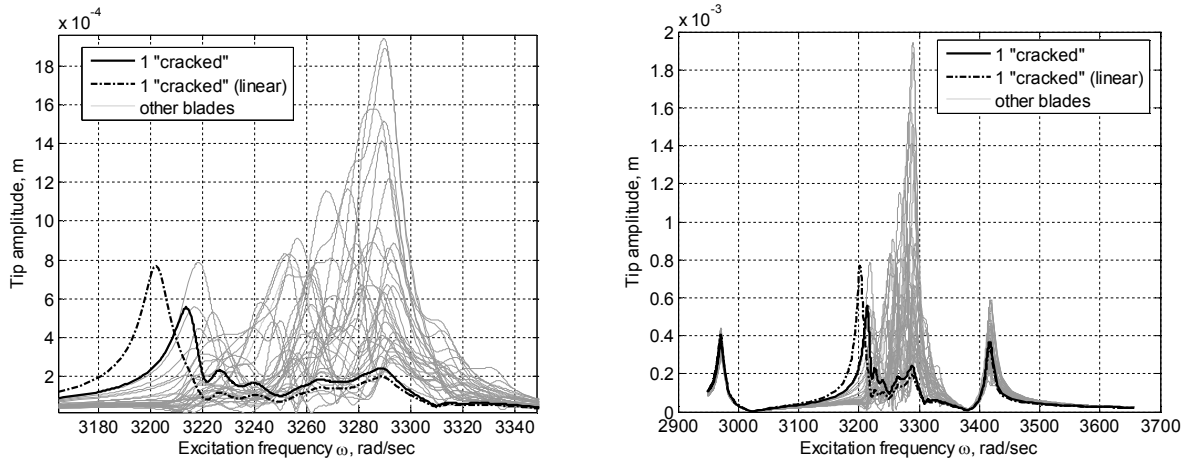

a b

Fig. 6. Mistuning effect on the bladed disk forced response (crack length a=4mm, EO=28):
a – σ=0.02; b – σ=0.02 (zoom)

The outcomes of simulations of different mistuning levels (figs. 5–6) have proved that the cracked blade nonlinear behavior taken into account arises difficulties in identification of the cracked blade. Sometimes it becomes impossible to distinguish a cracked blade localized dynamic behavior. The linear model at mistuning level of $\sigma = 0.02$ allows to recognize the cracked blade, whereas the nonlinear model makes the procedure unrealizable (fig. 6). The maximum of the cracked blade localized response depends on excitation force phase lag. The maximum of the cracked blade response increases with a raise of difference between numbers of stator and rotor blades. This can be explained by an increase of number of excited nodal diameters. In this case a decrease of coupling between neighboring blades occurs that results in more independent behavior of the frequency localized cracked blade. But this relationship is not always monotonic and depends on blade- and disk-dominated modes interaction and disk-blade mode veering location. In [9] it was shown that in the blade-dominated family of modes, the transfer of modal energy to the disk in veering results in a lower force exciting the mode as well as lower amplitude of blade.

With the cracked blade localization achieved, a particular case should be considered. It could be supposed that mistuning will be more critical for cracked blade detection under absence of the localization phenomenon.

Moreover, in such case it would be possible to omit the nonlinear formulation of cracked blade behavior. The initial data are as it was before, notwithstanding that the crack length decreased to 2mm (6.65% cracked blade). Figs. 9–10 are provided to show cracked blade detectability under the absence of the localization phenomenon.

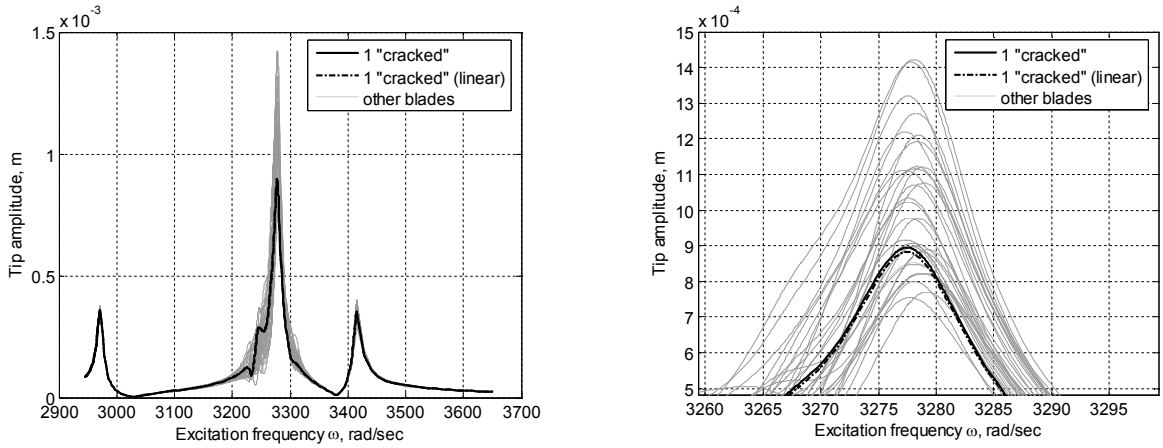

a b

Fig. 7. Mistuning effect on the bladed disk forced response (crack length a=2mm, EO=28): a – σ=0.005; b – σ=0.005 (zoom)

A conclusion can be drawn that under absence of the forced response localization even a relatively small level of the mistuning makes impossible to separate the cracked blade response from those of the rest of blades (fig. 7). Additionally, no resonance shift is observed by comparing results of the linear and nonlinear model solutions. Only a small difference in amplitude levels is seen between both model solutions under absence of mistuning. These observations allow the following use of the linear formulation of the crack presence in the blade under absence of localization of the cracked blade vibration.

Furthermore, it should be noted that additional resonances in the case of EO = 28 (figs. 5–7) are present, whereas they are absent when the excitation forces frequency lag (fig. 6) is not taken into account. These resonances correspond to disk-dominated modes of three nodal diameters and their excitation is explained by the rules of ZigZag diagram.

3. Simulations of tip-timing measurements

To continue with mathematical formulation of tip-timing method, some remarks should be declared. As far as our main task is simulation of tip-timing method application to cracked blade identification, some "raw" measurement data should be available. They are arriving times of each blade captured by probes. At absence of experimental data we need to create a database containing these data. It can be performed by establishing a relationship between arriving time of vibrating blade and parameters of its frequency response (amplitude and phase of vibration) depending on blade and probe angular position. Therefore the process of tip-timing method simulation will consists of two principal stages:

– blade arriving times generation (simulation of experimental measurements) to emulate real experiment

– reconstruction of blade tip amplitude and phase using arriving times with the goal to obtain bladed disk forced response.

3.1. Generation of the blade tip arriving times

Tip-timing method can be used for both single blade and for multi-blades measurements. Firstly, the approaches for one blade measurement simulation were developed [20].

Let's consider fig. 8. The blade rotates at speed Ω and passes each probe at one rotation. Then it is assumed that the origin is chosen such that the blade is at angular position ε at time t = 0. The time required for the blade without vibration to pass through the probe at k rotations is:

$$t_{uv} = \frac{\varepsilon + \phi}{\Omega} + \frac{2\pi k}{\Omega}, \qquad (3)$$

where Ω is the frequency of the rotor rotation at particular measurement, ε is the blade positioning angle relatively to the first blade at first probe and φ is the probe positioning angle counting from the first probe.

It will be accepted during consequent simulations that origin coincides with angular position of the first probe and the first measurement is attributed to the first blade.

During rotation each blade passes the following angular distances:

– to probe

$$c = \varepsilon + \phi + 2\pi k;$$

– due to rotation

$$d_r = \Omega t;$$

– due to vibration

$$d_v = \left[\frac{A(\omega)\sin(\omega t + EO\varepsilon + \psi(\omega))}{R} \right].$$

Accepting $c = d_r + d_v$, the governing equation of the blade tip-timing method will be derived to calculate the actual arriving time [7]:

$$\Omega t_k - (2\pi k + \varepsilon + \phi) + \left[\frac{A(\omega)\sin(\omega t_k + EO\varepsilon + \psi(\omega))}{R}\right] = 0, \quad (4)$$

where $A(\omega)$ and $\psi(\omega)$ are amplitude and phase obtained from forced response of bladed disk model developed in section 2, ω is the excitation frequency at particular measurement.

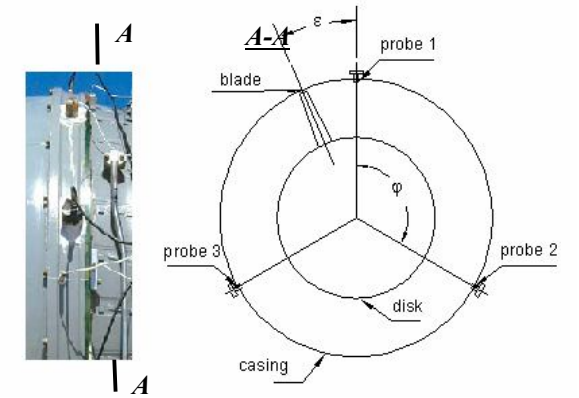

Fig. 8. Presentation of the tip-timing method

Equation (4) is solved by a method of nonlinear equations solution (Newton's method) in order to obtain tip arriving time of each vibrating blade at each probe.

The rotor speed is assumed to be constant at every point of the measurement; however the supposition is not longer valid. In the case of high frequency of rotor acceleration, the error in amplitude calculation will not be negligible. It means that the blade passes through probes at different frequencies of excitation and this can be avoided by decreasing rotor acceleration or approximation of the rotor acceleration curve by step-function.

Therefore the rotor speed should be maintained constant throughout every measurement, especially in the resonance area. The requirement can be fulfilled through the engine maintenance procedures aimed at determining the bladed disk vibration performances and detecting possible damages.

3.2. Blade tip amplitude reconstruction by tip-timing data

Tip-timing measurements of a blade are presented in fig. 9. The time-history curve of the blade is intersected by 3 trucking lines of each probe giving three values of the tip amplitude. The linear distance passed by tip of j-th blade without vibration is equal to $R\Omega t^i_{k,p}$, which is measured for p-th probe at k-th rotation of the working wheel (disk). Without vibration this distance will be constant. However, if the blade is subjected to vibration, it will be possible to capture arriving time difference and reconstruct the blade tip amplitude.

Numerical expression of the blade response captured by p-th probe using arriving time data can be written as follows:

$$a^j_{k,p} = R\Omega\Delta t^j_{k,p},\ j = 1...n_r,\ p = 1...n, \quad (5)$$

where $\Delta t^j_{k,p} = (t^j_{k,v} - t^j_{k,uv})_p$ is the arriving time difference between vibrating blade and blade without vibration, which is synchronized to impulse of the first blade without vibration captured at the origin of measurements (first probe).

Fig. 9 shows derivation of formula (5). There are curves of the blade tip time-history and tracking lines of three probes.

Since the probes are fixed and we are in the rotating reference frame, the tracking line of the probes will be opposite to direction of the rotor rotation. Segment DE represents amplitude of the blade tip vibration (fig. 9), whereas segment EF is the arriving time difference $\Delta t^i_{k,p}$ measured by a probe.

Equation (5) is easily drawn on base of this geometrical presentation.

Expression (5) enables calculation of the maximum tip amplitude of every blade [10], [11]. It has already been specified that there are n data points of the blade tip response (n – number of probes) at every rotation.

A tip response is supposed to sinusoidal (Fig. 6) and thus can be represented at point D (fig. 19, b) as:

$$a^j_p = A^j_k \sin(\omega_k t_{k,v} + \psi_k),\ j = 1...n_r,\ p = 1...1, \quad (6)$$

where A^j_k is the maximum amplitude of j-th blade tip in k-th measurement point and ψ_k is the phase.

In the case of three probes, equation (6) leads to a system of three equations with undefined A and ψ. For a blade at a particular frequency (measurement point) the system will be as:

$$\begin{cases} A\sin(\omega t_{1v} + \psi) = R\Omega(t_{1v} - t_{1uv}); \\ A\sin(\omega t_{2v} + \psi) = R\Omega(t_{2v} - t_{2uv}); \\ A\sin(\omega t_{3v} + \psi) = R\Omega(t_{3v} - t_{3uv}). \end{cases} \quad (7)$$

The system (13) can be rewritten in order to use the method of solving the system of linear equations:

$$\begin{cases} b\cos(\omega t_{1v}) + c\sin(\omega t_{1v}) = R\Omega(t_{1v} - t_{1uv}); \\ b\cos(\omega t_{2v}) + c\sin(\omega t_{2v}) = R\Omega(t_{2v} - t_{2uv}); \\ b\cos(\omega t_{3v}) + c\sin(\omega t_{3v}) = R\Omega(t_{3v} - t_{3uv}), \end{cases} \quad (8)$$

$$A = \sqrt{b^2 + c^2},\ \psi = \arctan(c/b).$$

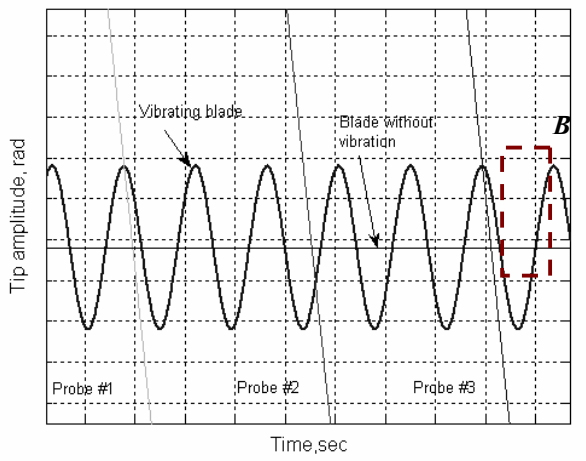

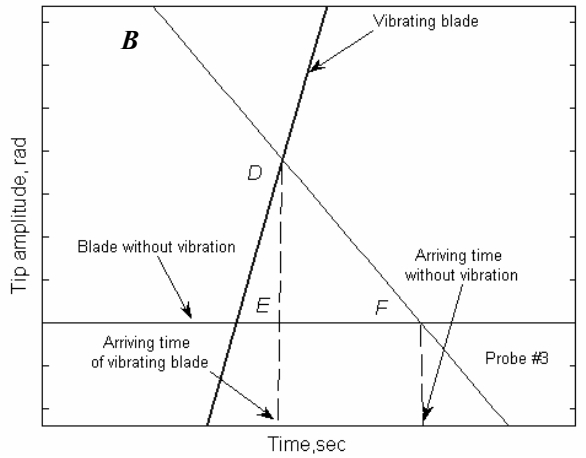

Fig. 9. Tim-timing measurements of a selected blade

Structurally, the blade tip amplitude reconstruction comprises the following stages:

– blade tip arriving time generation with and without vibration using equation (4);

– synchronizing arriving time to the arriving time of the first blade without vibration captured by the first probe;

– calculation of the blade tip amplitude captured by probe using formula (5);

– reconstruction of maximum blade tip amplitude and phase using system of equations (8).

Throughout simulation it is possible to make k measurements of each blade vibration state, which is equal to the rotor rotation number accomplished over time of the rotor acceleration:

$$k = \Omega_1 \mathrm{Tr} + \left(\frac{\Omega_2 - \Omega_1}{\mathrm{Tr}} \right) \frac{\mathrm{Tr}^2}{2} = \Omega_1 \mathrm{Tr} + (\Omega_2 - \Omega_1) \frac{\mathrm{Tr}}{2}, \quad (9)$$

where Ω_2, Ω_1 are the rotor rotation frequencies at the end and beginning of the rotor acceleration time, Tr is the rotor acceleration time. Rotation speed is supposed to be changed linearly at the rotor acceleration.

The initial data for the blade tip-timing method simulation:

– engine acceleration time – Tr = 5sec;
– rotor frequency range – Ω=16…20Hz;
– engine order of excitation – EO = 28;
– excitation force amplitude – F_a = 0.3N;
– rotor radius – R = 0.38m;
– number of measurements – k = 90;
– number of probes – n = 3.

For each of the simulation cases a comparison is made of the forced response obtained with the arriving time data and the forced response by harmonic balance method. The responses of all-blades response in particular measurement point (excitation frequency) are to be obtained in order to assess the feasibility of identifying a cracked blade. It also allows identification of a cracked blade by the tip amplitude distinction away from the resonance peak. An attention should be paid to the engine acceleration time, which is important to accurately represent frequency response curve of the investigated object. Some numerical tests were performed to verify correctness of the chosen value of the rotor acceleration time.

Figs. 10–11 show the outcomes of the tip-timing measurements at different levels of mistuning and also prove applicability of the blade tip-timing method to the blade tip amplitude measurements and construction of the bladed disk frequency response in the case of the cracked blade frequency localization (13.3% cracked blade.)

The results shown in figs. 10–11 confirm the supposition stated in 1.3: the mistuning level of σ = 0.02 makes identification of the cracked blade impossible, whereas it is achievable under the mistuning level of σ = 0.01. There is again a case of deterioration of detectability of the cracked blade under application of the nonlinear formulation of a cracked blade behavior. Earlier it has been shown that a cracked blade response at σ = 0.02 of mistuning at its linear formulation is still possible to distinguish, but the nonlinear formulation makes the procedure unfeasible (figs.5–6).

The tip-timing simulation allows making a comparison of the maximum amplitude responses of all blades at each point of the measurement (fig. 12–13). To demonstrate this, four points of measurement were selected: before the cracked blade localized response (fig. 12a), around the cracked blade localized response (fig. 12b), around the all-blades principal response (fig. 13a), after the all-blades principal response (fig. 13c). Each of the points is described by three curves showing the blade tip amplitude response calculated by the harmonic balance method (“by HB method”), using tip-timing method data with nonlinear (“by TTM data (nonlinear case)”) and linear formulation of the cracked blade behavior (“by TTM data (linear case)”).

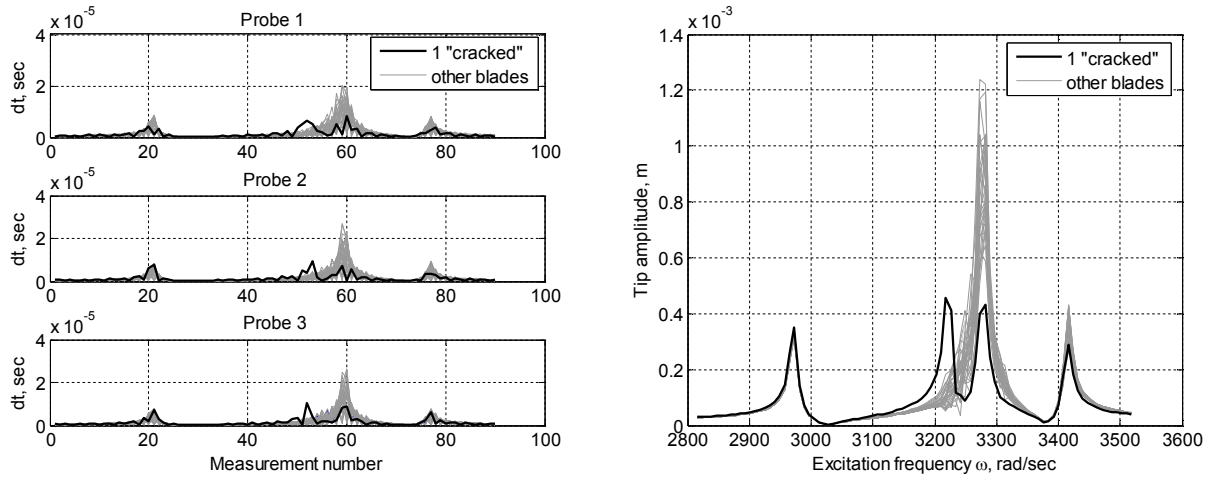

a b

Fig. 10. The results obtained by the blade tip timing method (crack length a=4mm (13.3% cracked blade), σ=0.01): a – arriving time differences "seen" on the probes; b – bladed disk forced response by TTM data

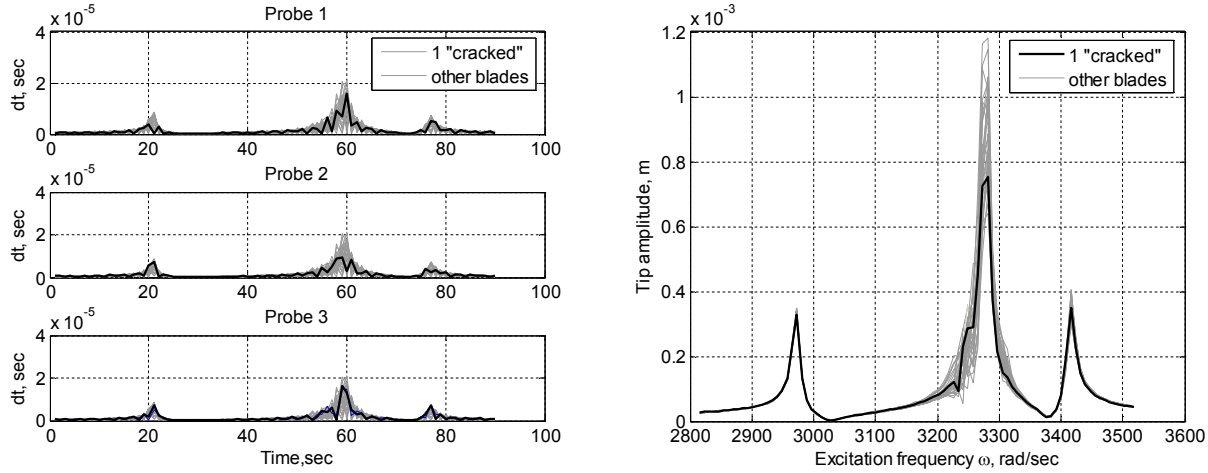

a b

Fig. 11. The results obtained by the blade tip timing method (crack length a=2mm (6.65% cracked blade), σ=0.005): a – arriving time differences "seen" on the probes; b – bladed disk forced response by TTM data

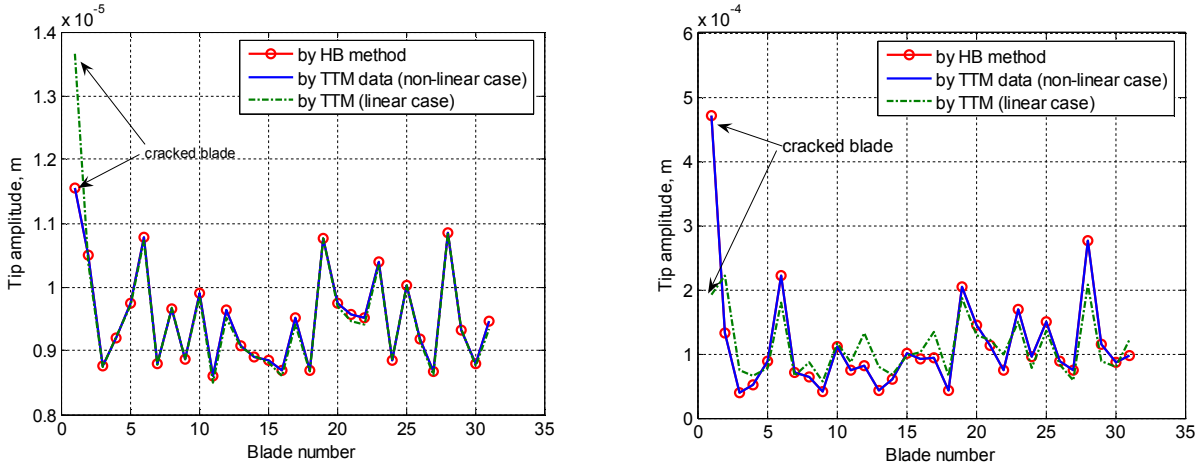

a b

Fig. 12. The all-blades response at the point of measurement (crack length a=4mm (13.3% cracked blade), σ=0.01): a – ω = 3044.2rad/sec; b – ω = 3218.1rad/sec

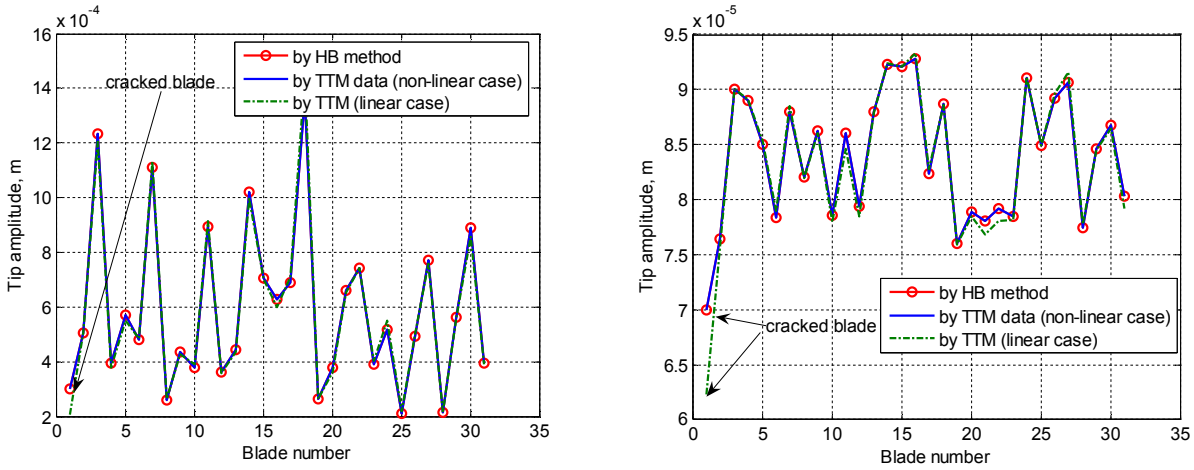

a b

Fig. 13. The all-blades response at the point of measurement (crack length *a*=4mm (13.3% cracked blade), σ=0.01): a – ω = 3273.5rad/sec; b – ω = 3455.3rad/sec

An analysis of the mistuned bladed disk response data at each point of the measurement reveals a decrease of the cracked blade detectability under presence of mistuning. In the case of mistuning level of σ = 0.01 (Fig. 12–13) it is still possible to distinguish an amplitude of the cracked blade tip almost at all points of measurement except for the point #59 (Fig. 13a.) This point is close to the all-blades resonance peak, which is the most mistuned one. A more detailed examination of distribution of the all-blades amplitudes shows that the cracked blade amplitude is the highest one before the all-blades principal response. A cracked blade is almost impossible to detect around it, though when the all-blades resonance frequency blades respond in a more structured manner, a cracked blade can be distinguished again. In this case the cracked blade amplitude has the lowest value among the other blades.

4. Conclusions

The study dealt with two main issues: (1) an effect of the cracked blade on the bladed disk dynamic behavior, and (2) detection of a cracked blade by tip-timing method.

Examination of the mistuning influence has shown that some of its levels are critical for detection of a cracked blade. Moreover, the cracked blade nonlinearity diminishes the cracked blade detectability because of a shift of its natural frequencies closer to the uncracked state and lower amplitude of the cracked blade. It was also shown that presence of mistuning makes hardly achievable the detection of a cracked blade under absence of its frequency localization.

It should be noted that the finite elements model of the bladed disk is the simplified one. The suggested technique of simulation of the cracked blade presence can be easily applied in relation to more complex and realistic models.

Advantages of the tip-timing method are obvious as it provides an overall control over all blades. Application of the method simulation enables:

– to control vibration state of every blade independently and, thus have a more full understanding of the engine dynamic state

– to calculate the blade tip amplitudes on the base of data delivered by the probes

– to calculate resonance frequencies

– to detect the localized cracked blade in the assembly

Some problems can arise during implementation of the health monitoring system based on the tip-timing method. They can be grouped round impact of the low crack on overall blade dynamic performances. This phenomenon depends directly on the crack size and location in the blade and order of the excited eigenmode. The measurement system (probe) time resolution was also proved to be a very important parameter. The higher the time resolution is required with an increase of the excited eigenmode order and a decrease of magnitude of the blade tip amplitude.

References

1. Bladh R. Component-Mode-Based Reduced Order Modeling Techniques for Mistuned Bladed Disks – Part I: Theoretical models / R. Bladh, M. Castanier, C. Pierre // ASME Journal of Engineering for Gas Turbines and Power. – 2001. – Vol. 123(1). – P. 100-108.

2. Beauseroy P. Nonintrusive turbomachine blade vibration measurement system / P. Beauseroy, R. Lengelle // Mechanical Systems and Signal Processing. – 2007. – Vol. 21. – P. 1717-1738.

3. Cheng S. Vibrational response of a beam with a breathing crack/ S. Cheng, X. Wu, W. Wallace, A. Swamidas // Journal of Sound and Vibration. – 1999. – Vol. 225. – P. 201-208.

4. Craig R. Coupling of substructures for dynamic analysis/ R. Craig, M. Bampton // AIAA Journal. – 1968. – Vol. 6(7). – P. 1313-1319.

5. Dimitriadis G. Blade-tip timing measurement of synchronous vibrations of rotating bladed assemblies/ G. Dimitriadis, I. Carrington // Mechanical Systems and Signal Processing. – 2002. – Vol. 16(4). – P. 599-622.

6. Douka E. Time-frequency analysis of the free vibration response of a beam with a breathing crack / E. Douka, L. Hadjileontiadis // NDT&E International. – 2005. – Vol. 38 – P. 3-10.

7. Ghoshal A. Structural health monitoring techniques for wind turbine blades/ A. Ghoshal, M. Sundaresan, M. Schulz // Journal of Wind Engineering and Industrial Aerodynamics. – 1999. – Vol. 85. – P. 309-324.

8. Heath S. An improved single-parameter tip-timing method for turbomachinery blade vibration measurements using optical laser probes / S. Heath, M. Imregun // International Journal of Mechanical. – 1996. – Vol. 38 (10). – P. 1047-1058.

9. Kenyon J. Sensitivity of Tuned Bladed Disk Response to Frequency Veering/ J. Kenyon, J. Griffin, N. Kim // ASME Journal of Engineering for Gas Turbines and Power. – 2005. – Vol. 127(4). – P 835-842.

10. Kucher O. GTE blade vibration characteristics determination by non-contact method / O. Kucher, V. Kharyton // Visnyk NAU (Scientific review of National Aviation University). – 2007. – Vol. 1(31). – P. 134-138.

11. Kucher O. Vibrational diagnosing of GTE working wheel blades by blade tip-timing method / O. Kucher, V. Kharyton, J.-P. Laine, F. Thouverez // Proceedings of the international scientific conference AVIA-2007. – Kiev, Ukraine.

12. Kulyk M. Nonlinear analysis of the cracked blade in dynamics / M. Kulyk, O. Kucher, V. Kharyton, J.-P. Laine, F. Thouverez // Aviation. – 2008. – Vol. 12(3). – P. 66-79.

13. Laine J.-P. 2006 Cracked structure response on external harmonic excitation / J.-P. Laine // Aerospace technique and technology. – Vol. 61. – P. 1057-1074.

14. Lawson C. Tubomachinery blade vibration amplitude measurement through tip timing with capacitance tip clearance probes / C. Lawson, P. Ivey // Sensors and Actuators. – 2005. – Vol. 118. – P. 14-24.5

15. Rivas-Guerra J. Local Global effects of mistuning on the forced response of bladed disks / J. Rivas-Guerra, M. Mignolet // ASME Journal of Engineering for Gas Turbines and Power – Vol. 126 – P. 131-141.

16. Ruotolo R. Harmonic analysis of the vibrations of a cantilevered beam with a closing crack / R. Ruotolo, C. Surace, P. Crespo, D. Storer // Computers and Structures. – 1996. – Vol. 61. – P. 1057-1074.

17. Roy N. Helicopter rotor blade frequency evolution with damage growth and signal processing/ N. Roy, R. Ganguli // Journal of Sound and vibration. – 2000. – Vol. 283. – P. 821-851.

18. Saito A. Effects of a Cracked Blade on Mistuned Turbine Engine Rotor Vibration / A. Saito, M. Castanier, C. Pierre // ASME Paper DETC2007-35663, Proceedings of the ASME DETC2007. – Las Vegas, NV, USA.

19. Wildheim S. Excitation of rotationally periodic structures / S. Wildheim // Transaction of ASME. – 1979. – Vol. 46. – P. 878-883.

20. Zablotsky Y. Measurement of resonance vibrations of turbine blades with the ELURA device / Y. Zablotsky, Yu. Korostelev // Energomashinostroneniye. – 1970. – Vol. 2. – P. 36-39.

21. Zielinski M. Noncontact blade vibration measurement system for aeroengine application / M. Zielinski, G.. Ziller // International Symposium of Air Breathing Engines, ISABE-2005.

22. Zielinski M. Noncontact vibration measurements on compressor rotor blades / M. Zielinski, G. Ziller // Measurements Science and Technology. – Vol. 11. – 2000. – Vol. 847-856.

Поступила в редакцию 1.06.2009

Рецензент: д-р техн. наук, профессор В.В. Панин, Национальный авиационный университет, Киев, Украина.

ВИЗНАЧЕННЯ ЛОПАТКИ З ТРІЩИНОЮ З ВІДГУКУ ОБЛОПАЧЕНОГО ДИСКУ ЗА ДОПОМОГОЮ ТИП-ТАЙМІНГ МЕТОДУ: МОДЕЛЮВАННЯ

О.Г. Кучер, В.В. Харитон, Ж.-П. Лане, Ф. Тоуверез

Робота направлена на моделювання процесу розрахунку закінцівки лопатки тип-таймінг методом. Увага приділена процесу визначення наявності лопатки з тріщиною з відгуку облопаченого диску за рахунок моделювання вимірів тип-таймінг методу. Лопатка з тріщиною розглянута в рамках моделі облопаченого диску, яка здатна враховувати розбіжність структурних властивостей лопаток. Нелінійна модель тріщини реалізована за допомогою метода гармонічного балансу з елементами контактного аналізу. Для забезпечення

більшої наглядності процесу визначення наявності лопатки з тріщиною, розмір та розташування тріщини вибрані такими, які забезпечують частотну локалізацію лопатки з тріщиною. Реконструкція амплітуд закінцівок лопаток виконана, використовуючи час проходженні лопаткою стаціонарно встановлених датчиків. Здійснено порівняння результатів за даними отриманими з АЧХ моделі облопаченого диску. Запропонована модель може бути використана для моделювання процесу моніторингу технічного стану авіаційних газотурбінних двигунів. Зокрема, для забезпечення інформацією про зміну параметрів вібраційного стану в експлуатації.

Ключові слова: лопатка з тріщиною, облопачений диск, АЧХ облопаченого диску, тип-таймінг метод.

ОПРЕДЕЛЕНИЕ ТРЕЩИНЫ ИЗ ОТКЛИКА ОБЛОПАЧЕННОГО ДИСКА ПОСРЕДСТВОМ ТИП-ТАЙМИНГ МЕТОДА: МОДЕЛИРОВАНИЕ

А.Г. Кучер, В.В. Харитон, Ж.-П. Ланэ, Ф. Тоуверез

Работа направлена на моделирование процесса расчета амплитуды законцовки лопатки посредством тип-тайминг метода. Внимание уделено моделированию замеров тип-тайминг методом с целью определения наличия лопатки с трещиной исходя из отклика облопаченного диска. Лопатка с трещиной рассмотрена в рамках модели облопаченного диска, которая способна учитывать разброс структурных свойств лопаток. Нелинейная модель трещины реализована при помощи метода гармонического баланса совместно с элементами контактного анализа. Для обеспечения большей наглядности процесса определения наличия лопатки с трещиной, размер и расположение трещины выбраны такими, что обеспечивают частотную локализацию лопатки с трещиной. Реконструкция амплитуд законцовок лопаток выполнена за счет использования времени прохождения лопаткой стационарно установленных датчиков. Произведено сравнение результатов с данными полученными из АЧХ модели облопаченного диска. Предложенная модель может быть использована для моделирования процесса мониторинга технического состояния авиационных газотурбинных двигателей. В частности, для обеспечения информацией об изменении параметров вибрационного состояния в эксплуатации.

Ключевые слова: лопатка с трещиной, облопаченный диск, АЧХ облопаченного диска, тип-тайминг метод.

Кучер Алексей Григорьевич – д-р техн. наук, профессор, профессор кафедры авиационных двигателей Национального авиационного университета, Киев, Украина, e-mail: kucher@nau.edu.ua.

Харитон Всеволод Владимирович – PhD, инженер, Лионская высшая центральная школа, Лаборатория трибологии и динамики систем, Лион, Франция / кафедра авиационных двигателей Национального авиационного университета, Киев, Украина, e-mail: vsevolod.kharytonr@gmail.com.

Жан-Пьер Лане – PhD, доцент, Лионская высшая центральная школа, Лаборатория трибологии и динамики систем, Лион, Франция, e-mail: jean-pierre.laine@ec-lyon.fr.

Фабрис Тоуверез – PhD, профессор, Лионская высшая центральная школа, Лаборатория трибологии и динамики систем, Лион, Франция, e-mail: fabrice.thouverez@ec-lyon.fr.